

In-situ SAXS-WAXS study on preparation of activated carbon from anthracite

Xia Li<sup>1,2</sup>, Yueqian Fan<sup>2,1</sup>, Zhihong Li<sup>1\*</sup>

<sup>1</sup> Beijing Synchrotron Radiation Facility, Institute of High Energy Physics, Chinese Academy of Sciences, Beijing 100049, China

<sup>2</sup> State Key Laboratory of Clean and Efficient Utilization of Coal-based Energy, Taiyuan University of Technology, Taiyuan 030024, China

Received February 3, 2025; Accepted May 12, 2025

---

## Abstract

Activated carbon is a carbon material with good adsorption and catalytic properties, and coal is the primary raw material for its production. In this study, anthracite is used as the raw material, and carbon dioxide is used as the activating agent to prepare activated carbon. Utilizing synchrotron in-situ small-angle X-ray scattering (SAXS) and wide-angle X-ray scattering (WAXS) simultaneous measurement techniques, the entire continuous process of carbonization, activation, and cooling during activated carbon preparation is monitored in situ, revealing changes in pore and carbon skeleton structures. The results show that the preparation process of anthracite-based activated carbon exhibits distinct stages, with pore structure changes including the expansion of micropores, and the formation of mesopores and macropores. The specific surface area increases significantly, and the degree of graphitization of the carbon skeleton increases with rising temperature, while the lamellar stacking height and lamellar lateral size gradually decrease. The finally prepared activated carbon possesses a developed pore network structure and high specific surface area, providing a structural foundation for improving its adsorption performance.

**Keywords:** Anthracite; Activated carbon; Microstructure; Small-angle X-ray scattering (SAXS); Wide-angle X-ray scattering (WAXS).

---

## 1. Introduction

Activated carbon is a porous material widely used in fields such as adsorbents, electrode materials, and catalysts [1]. Among them, coal-based activated carbon is one of the main types, favored for its abundant raw material sources, low production cost, high adsorption efficiency, strong tunability, and good high-temperature resistance [1]. The organic matter core of coal consists of aromatic rings, and the higher the coal rank, the more complete its graphitic microcrystalline structure [2]. The arrangement of aromatic groups and functional groups in coal forms pores, making coal a porous substance [2]. Various types of coal can be used to prepare activated carbon [1]. Anthracite, a high-rank coal, is particularly noteworthy due to its high carbon content and low volatile matter content, and the activated carbon prepared from it exhibits high purity, uniform pore structure, high adsorption efficiency, high stability, and renewability [2]. The micropore specific surface area constitutes the majority of the activated carbon's surface area and largely determines its adsorption capacity. Mesopores provide adsorption sites for larger molecules that cannot enter micropores, causing capillary condensation at higher relative pressures. Macropores serve mainly as channels for adsorbate molecules to reach micropores and mesopores, having little impact on the adsorption process [3].

The primary processes for preparing activated carbon from coal include carbonization and activation [3]. Carbonization involves the low-temperature pyrolysis of coal, heating it to about 500-600°C in an inert atmosphere to remove volatile matter, reduce non-carbon elements, and form char (semi-coke). During this process, non-carbon elements are released as coal

gas and tar, leaving behind a carbon atom framework that forms the initial pore structure, the precursor of activated carbon. Activation, often achieved through physical activation, involves heating the char to 800-1000°C in an oxidizing atmosphere, where multi-phase reactions further etch the char framework, remove tar substances and uncarbonized material, open blocked pores, enlarge existing pores, and create new ones, thus forming a developed pore structure, increasing specific surface area and activity. The commonly used carbon dioxide activation method focuses more on pore development, especially the formation of microporous structures. The narrow micropore size distribution tends to have molecular sieve properties, thereby enhancing the adsorption capacity and catalytic efficiency of the activated carbon [1].

Coal and activated carbon have always been focal points in carbon material research [2]. However, producing high-performance activated carbon from coal remains a challenging task. Despite extensive research on coal and activated carbon, understanding the structural transformation characteristics and mechanisms of coal-based activated carbon preparation is still inadequate, primarily due to the complexity of the system structure and the lack of powerful in-situ characterization techniques.

Coal and activated carbon are common porous materials [2], suitable for studying their pore and skeleton structures using small-angle X-ray scattering (SAXS) and wide-angle X-ray scattering (WAXS) [5-7]. SAXS can measure pore structure, such as specific surface area, porosity, pore size, and distribution, and assess the electron density heterogeneity and interface blurriness in samples [8]. Compared to other methods [9], SAXS sample preparation is simple, suitable for both dry and wet samples, and provides statistical structural information. WAXS measures graphitic microcrystalline structures, including lamellar spacing, lamellar lateral size, and lamellar stacking height [10]. The information is crucial for understanding the structure and performance of coal and activated carbon.

SAXS and WAXS have been widely used in static structural studies of coal and activated carbon [11-13], as well as in a few dynamic studies on coal carbonization [14-16], but there have been no reports of their use in in-situ studies of the entire preparation process of coal-based activated carbon, including carbonization and activation. This study, based on advanced synchrotron facilities, uses SAXS-WAXS simultaneous measurement techniques to conduct in-situ studies on the entire continuous process of carbonization, activation, and cooling during activated carbon preparation from coal, obtaining information on simultaneous changes in pore and carbon skeleton structures.

## 2. Experiment

### 2.1. Raw material

The raw material for the coal-based activated carbon in this study is anthracite, sourced from the Zhaogu No. 2 Mine in Jiaozuo, Henan Province, China. To evaluate the coal quality, proximate and ultimate analyses were performed on the raw coal. These tests were completed at the Shanxi Institute of Coal Chemistry, Chinese Academy of Sciences.

### 2.2. In-situ SAXS-WAXS

A small piece of raw coal was polished into a thin circular slice with a diameter of about 10 mm and a thickness of 1 mm for in-situ testing. The in-situ heating furnace for the sample was self-developed by us [17].

The in-situ simultaneous SAXS-WAXS testing during the preparation of activated carbon from anthracite was conducted at the SAXS experimental station of the 1W2A beamline at the Beijing Synchrotron Radiation Facility (BSRF) [18], as shown in Figure 1. During the experiment, the electron beam energy in the storage ring was 2.5 GeV, the electron beam current was 250 mA, the injection mode was up-top, the incident X-ray wavelength was 0.154 nm, and the photon flux at the sample position was approximately  $5.5 \times 10^{11}$  phs/sec. The SAXS detector used was a Pilatus 1MF, with a beam spot size of  $1.4 \times 0.2$  mm<sup>2</sup> on the detector, and the sample-to-detector distance was 1749 mm. The WAXS detector was a Mar165 CCD, placed at an angle, i.e., the detector was inclined at 79.70° relative to the direct beam. This setup

increased the measurable angle range, high-angle intensity, and statistical accuracy. The vertical distance from the sample to the detector was 48.53 mm, and the distance along the beam path from the sample to the lower end of the detector was 221.41 mm. This configuration allowed the measurement of the  $2\theta$  angle range from  $12.66^\circ$  to  $48.38^\circ$ .

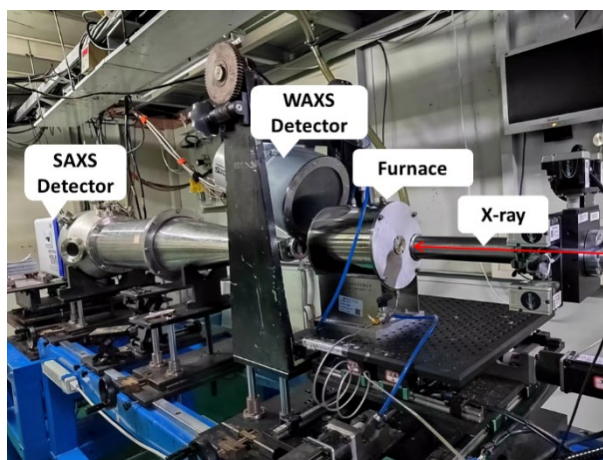


Figure 1. Photo of the in-situ SAXS-WAXS experiment for the preparation of activated carbon from anthracite conducted at the SAXS experimental station of the 1W2A beamline at the Beijing Synchrotron Radiation Facility (BSRF).

The sample was heated from room temperature to  $600^\circ\text{C}$  under a nitrogen atmosphere and then carbonized by holding at  $600^\circ\text{C}$  for 1 hour. Next, carbon dioxide was introduced, nitrogen was stopped, and the temperature was raised to  $900^\circ\text{C}$  for 1 hour of activation. The sample was then naturally cooled to room temperature under a carbon dioxide atmosphere. Throughout the process, the gas flow rate was 1 L/min, and the heating rate was  $10^\circ\text{C}/\text{min}$ . During the heating process, an exposure was taken every  $25^\circ\text{C}$  increase in temperature, every 2 minutes during the holding period, and every  $25^\circ\text{C}$  decrease during the cooling process, with each exposure lasting 5 seconds. Standard samples SRM 3600 glassy carbon and polypropylene were tested under the same geometric conditions, each with a 5-second exposure time. The former was used to calibrate the absolute scattering intensity and angle of SAXS [19], and the latter to calibrate the WAXS angle [20]. Data processing involved using Fit2d software [21] to convert SAXS and WAXS two-dimensional images into one-dimensional curves through rectangular integration; using S.exe software [22] to normalize SAXS data, subtract the background, and calculate porosity, specific surface area, and fractal dimension; using McSAS software [23] to calculate pore distribution; and using OriginPro2021 software to subtract the background and fit WAXS peaks.

### 2.3. Apparent density

The apparent density of coal, char, and coke refers to the actual mass per unit volume of the solid, excluding the volume of pores and cracks [24-25]. Approximately 10 g of raw coal powder with a particle size of  $<1$  mm was taken, and using the same heating furnace as for the in-situ tests, it was heated to  $100^\circ\text{C}$ ,  $300^\circ\text{C}$ ,  $500^\circ\text{C}$ ,  $700^\circ\text{C}$ , and  $900^\circ\text{C}$  at the same heating rate under the same gas flow rate, then naturally cooled to room temperature to produce several offline samples at respective temperatures. After drying them in a  $60^\circ\text{C}$  oven for 12 hours, they were used for apparent density testing. The apparent density tests were completed at the Beijing Physical and Chemical Analysis Testing Center using an AccuPyc 1330 fully automatic apparent density analyzer with helium displacement method. The true densities at other temperatures were obtained by interpolation. The true densities of these offline samples were used to approximate the true densities of the corresponding products during the in-situ process at respective temperatures.

## 2.4. Nitrogen adsorption

To characterize the pore structure of the raw material and products and to compare with SAXS structural data, nitrogen adsorption experiments were conducted on raw coal and offline-prepared activated carbon sample. Approximately 2 g of raw coal powder with a particle size smaller than 1 mm was used to prepare offline activated carbon samples in a tubular furnace (OTF-1200X-S) following the same procedure as the in-situ experiments. The experiments were carried out on the Syanjia Lab (<https://www.shiyanjia.com/>) using a Micromeritics ASAP 2460 physical adsorption analyzer. The adsorption gas was nitrogen (77 K), with a degassing temperature of 200°C and a degassing time of 8 hours.

## 3. Results and discussion

### 3.1. Properties of raw material and products

Table 1 presents the proximate and ultimate analysis results of the raw coal. This coal has a low volatile matter content and a high fixed carbon content, indicating that it is highly metamorphosed. According to the classification principles of China's national standard for coal classification, "GB5751-86," the volatile matter ( $V_{daf}$ ) <10% shown in Table 1 classifies this sample as typical highly metamorphosed anthracite. Anthracite is a high-rank coal characterized by high carbon content, low ash, and low volatile matter content [21].

Table 1. Proximate and ultimate analysis results of anthracite from Zhaogu No. 2 Mine.

Proximate analysis		Ultimate analysis (ad, %)	
Moisture (ad, %)	0.95	C	74.07
Ash (ad, %)	18.2	H	1.81
Fixed carbon (daf, %)	94.12	O	1.83
Volatile matter (daf, %)	5.88	N	0.62
Caking index	2	S	2.53

Table 2. Apparent density of offline samples of anthracite tested at different temperatures.

Temperature (°C)	100	300	500	700	900
Apparent density (g/cm <sup>3</sup> )	1.801	1.829	1.814	1.825	2.001

Table 2 presents the apparent density results of the offline samples of anthracite tested at different temperatures. Before heating to 300-500°C, the decomposition of volatile matter and the generation of some tar cause a certain degree of weight loss in the coal, and the apparent density slightly decreases. After 500°C, the char undergoes further volumetric shrinkage to form coke. When carbon dioxide is introduced into the system, the surface material of the sample first reacts with carbon dioxide. At the initial stage of activation at 700°C, the carbon structure is relatively stable, and the apparent density slightly increases. With further activation, the degree of graphitization decreases first and then increases, a large number of pores form internally, a transformation of pores from closed one to open one, leading to a significant increase in apparent density. The apparent density results are used to calculate the porosity and specific surface area of the samples [26-27].

Although this study focuses on in-situ SAXS experiments during the carbonization and activation processes, no direct measurements of carbonization and activation yields were performed. However, relevant data are available in the literature for anthracite-based activated carbon prepared under similar carbonization conditions. The carbonization yield is reported to be 91.67% [28]. As for activation, the reported activation yield is 43.44%, though this value was obtained using steam as the activating agent, rather than carbon dioxide as in this study [28].

It is well-known that steam is a stronger activating agent compared to carbon dioxide under similar conditions, leading to higher porosity and activation yields. In contrast, carbon dioxide provides a milder activation effect, which can better balance micropore and mesopore development. These differences underline the exploratory nature of this study in investigating the

structural evolution during CO<sub>2</sub> activation and its potential to yield activated carbons with unique characteristics.

### 3.2. In-situ SAXS

Some of the SAXS curves during the preparation of activated carbon from anthracite are shown in Figures 2 and 3 as double logarithmic plots and Porod plots, respectively. The pores in the samples are the primary scatterers, and the scattering curves mainly reflect the changes in pore structure within the samples [13,29]. Almost all scattering curves in Figure 2 exhibit linear segments in both the low- $q$  and high- $q$  regions. Based on the slope analysis [29-30], these segments correspond to surface fractals and pore fractals, respectively, with the changes in fractal dimensions shown in Figure 4.

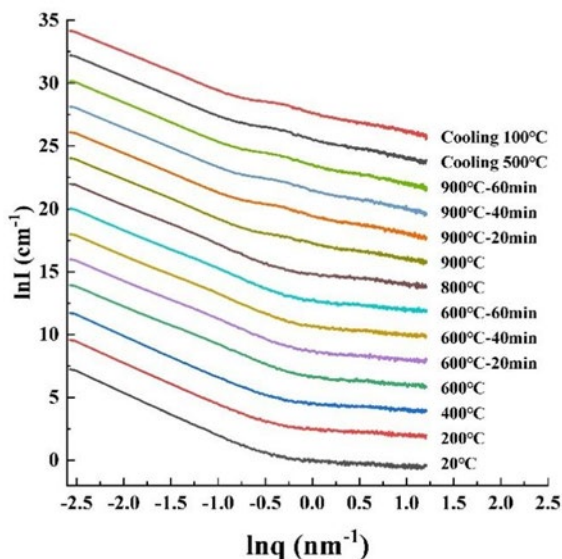


Figure 2. Double logarithmic scattering curves of in-situ SAXS at several temperatures during the preparation of activated carbon from anthracite (curves have been shifted vertically for clarity).

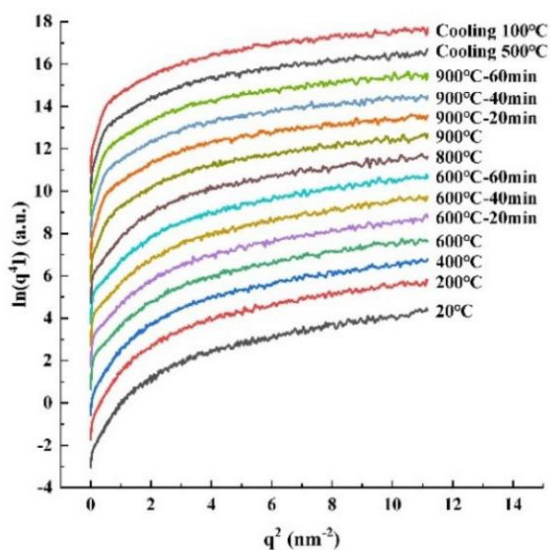


Figure 3. Changes in the Porod curves of in-situ SAXS at several temperatures during the preparation of activated carbon from anthracite (curves have been shifted vertically for clarity).

It can be seen that surface fractals and pore fractals are present throughout the entire preparation process, indicating that a rich pore network structure and carbon matrix organization are formed in the system. The pore network and its surfaces exhibit self-similarity and scale-invariant complex structural characteristics. From the raw anthracite to the final product activated carbon, the surface fractal dimension increased from 2.69 to 2.92, and the pore fractal dimension increased from 0.45 to 1.42, indicating that the pore network structure gradually becomes more developed, and the pore surface becomes rougher, which is beneficial for enhancing the adsorption activity of the product. During the activation stage, when the temperature reaches 900°C, the scattering curves show a diffuse hump around  $\ln q$  from  $-0.7 \text{ nm}^{-1}$  to  $0.2 \text{ nm}^{-1}$ , indicating a weakly ordered trend in the arrangement of channels with a spacing of approximately 12.76 nm.

All scattering curves in Figure 3 exhibit positive deviations from Porod's law, indicating that the skeleton structure of the raw material, intermediates, and products is heterogeneous [22,31-32], the carbonization is incomplete, and both graphitic microcrystalline and amorphous components coexist. Impurities (adsorbate) also remain in the pores, creating micro electron density fluctuations. These fluctuations generate additional scattering, superimposed on the scattering from the main scatterers, the pores, resulting in overall positive deviations from Porod's law. The degree of deviation can be quantitatively expressed by the slope of the deviation. By correcting for the positive deviation [33], the scattering data of the pores can be obtained,

allowing for the analysis of the pore structure, including porosity, specific surface area, and pore size distribution.

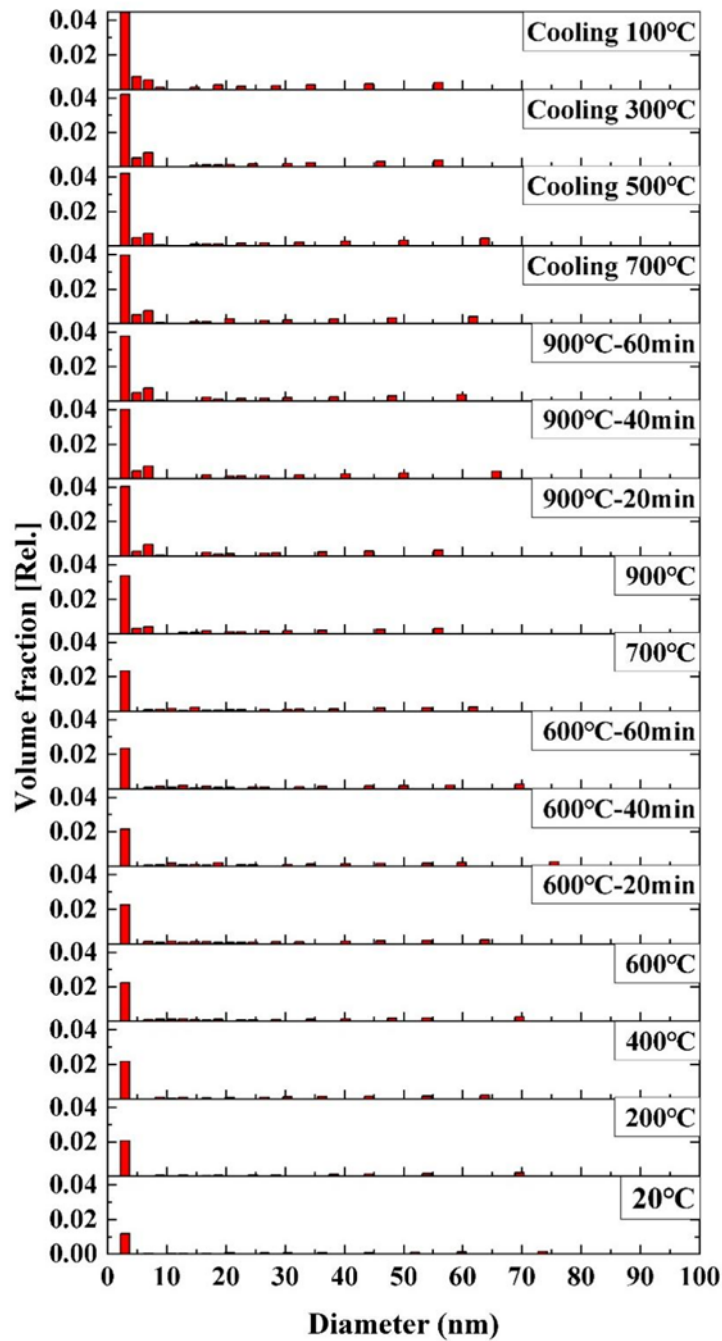


Figure 4. In-situ pore size distribution at several temperatures during the preparation of activated carbon from anthracite.

The SAXS analysis results are shown in Figures 4 and 5. From the pore size distribution histogram in Figure 4, changes in pore size can be observed. After the activation process begins, the content of micropores increases significantly, and mesopores gradually develop during the holding stage, indicating that carbon dioxide continuously etches the carbon skeleton structure to create pores throughout the activation process, further expanding the pores through newly formed channels, and maintaining the overall pore structure stability during

the cooling process. The fluctuations in the curves in Figure 5 reflect the destruction and formation of pores throughout the reaction process.

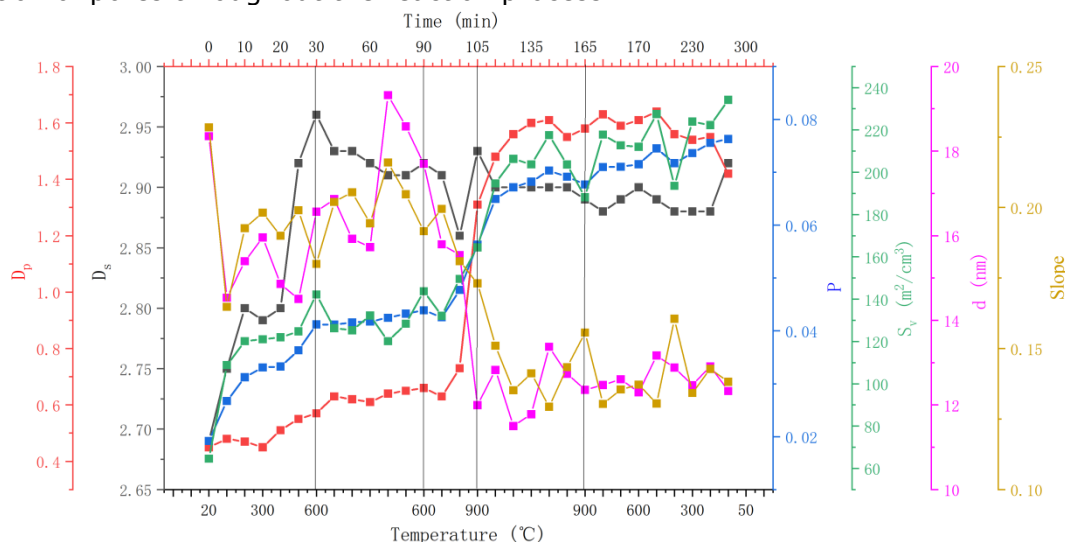


Figure 5. In-situ changes of SAXS structural parameters at several temperatures during the preparation of activated carbon from anthracite. Parameters include porosity ( $P$ ), specific surface area ( $S_v$ ), fractal dimensions (describing surface  $D_s$  and spatial complexity  $D_p$ ), and average pore size ( $d$ ), and slope of positive deviation from Porod's law (Slope).

From the raw anthracite to the final activated carbon product, within the measurable range of this experiment, the pore size distribution spans from 2.98 nm to 100 nm, namely covering small pores, mesopores, and some macropores. The smallest pores are the most developed, with the most probable size around 3 nm. The content of small pores, mesopores, and macropores all increase, the average pore size decreases from 18.35 nm to 12.33 nm, the porosity increases from 0.019 to 0.076, and the specific surface area increases from 64.58  $\text{m}^2/\text{cm}^3$  to 234.23  $\text{m}^2/\text{cm}^3$ . This indicates that the pore network structure becomes more developed, and the specific surface area substantially increases, enhancing the adsorption activity, successfully converting anthracite into activated carbon. The method for calculating SAXS structural parameters is detailed in the literatures [8,22]. The changes in SAXS structural parameters are discussed in detail below.

The structural parameters derived from SAXS analysis include porosity ( $P$ ), specific surface area ( $S_v$ ), fractal dimensions ( $D$ ), and average pore size ( $d$ ). Porosity represents the fraction of voids within the sample, indicating the extent of pore development. Specific surface area quantifies the surface area available for adsorption, which is critical for material performance. Fractal dimensions describe the complexity of the pore surfaces (surface fractal dimension  $D_s$ ) and the spatial arrangement of pores (pore fractal dimension  $D_p$ ). Average pore size characterizes the dominant pore size, reflecting the interplay between micropores, mesopores, and macropores formed during the activation process.

### 3.3. In-situ WAXS

Figure 6 shows the in-situ WAXS curves at several temperatures during the preparation of activated carbon from anthracite. The scattering curves mainly reflect the changes in the carbon skeleton structure within the samples [5]. From the WAXS curves, the broad and high peak between  $20^\circ$  and  $30^\circ$  represents the (002) peak of graphitic microcrystals in coal [10]. Graphitic microcrystals are composed of several stacked aromatic ring layers [2]. The higher and sharper the peak, the greater the aromatic carbon layer stacking height and the smaller the interlayer spacing, indicating a more regular and oriented arrangement of the layers. The asymmetry of the peak mainly arises from the superimposed influence of the  $\gamma$  peak and  $n$  peak at low angles, produced by carbon microcrystals attached to various alkyl side chains and functional groups connected to the aromatic rings [2]. The lower diffuse peak between  $40^\circ$

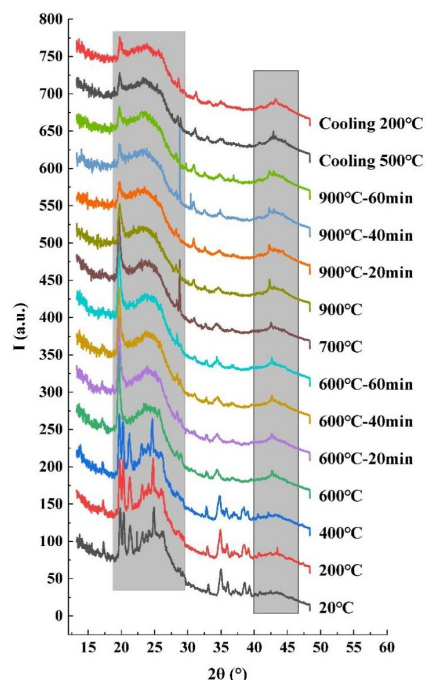


Figure 6. In-situ WAXS curves at several temperatures during the preparation of activated carbon from anthracite (curves have been shifted vertically for clarity).

The WAXS-derived structural parameters provide detailed insights into the evolution of the carbon skeleton. Lamellar spacing ( $d_{002}$ ) reflects the degree of graphitization and structural ordering of graphite-like microcrystals, with smaller values indicating more compact and ordered structures. Lamellar stacking height ( $L_c$ ) describes the crystalline dimensions along the c-axis, representing the vertical stacking height of aromatic layers. Lamellar lateral size ( $L_a$ ) represents the in-plane crystalline size of aromatic layers. Degree of graphitization ( $g$ ) quantifies the proportion of graphitic carbon, serving as an indicator of the structural order of the carbon skeleton.

### 3.4. Carbonization

In this study, the basic carbonization process involves heating anthracite from room temperature to 600°C under an inert nitrogen atmosphere, followed by one hour hold to produce char. The inert atmosphere prevents the oxidation and combustion of anthracite. As shown in Figures 5 and 7, the carbonization process of anthracite can be roughly divided into four stages: physical desorption, mild thermal decomposition, intense thermal decomposition, and thermal condensation.

(1) **Physical desorption:** At approximately 20~100°C, anthracite undergoes physical desorption, releasing free gases, adsorbed gases, and most of the external moisture (free water) within the pores [1,3], exposing a rough surface and freeing some pores. The proportion of small pores increases, the average pore size decreases, and the surface fractal dimension, pore fractal dimension, porosity, and specific surface area all increase. The release of gases and steam rapidly reduces electron density fluctuations within the pores, significantly decreasing the Porod slope. Due to thermal vibrations, lamellar spacing and lamellar stacking height increase, the layers become more relaxed, lamellar lateral size increases, and graphitization degree decreases as lamellar spacing increases.

(2) **Mild thermal decomposition:** At approximately 100~200°C, anthracite continues to release adsorbed gases and begins mild thermal decomposition, releasing carbon dioxide and some bound water [1,3], producing a small number of small pores, and opening up individual

and 50° represents the (100) peak of graphitic microcrystals in the sample, reflecting the size of the aromatic carbon layers [10]. The higher and sharper this peak, the larger the diameter of the microcrystalline aromatic carbon layers, and the higher the degree of aromatic ring condensation. The few distinct narrow and sharp peaks on the WAXS curves are diffraction peaks of minerals [10], which significantly decrease above 600°C due to the decomposition of minerals. After correcting the background of the WAXS curves, they can be used to calculate the structural parameters of graphitic microcrystals in the sample skeleton, including the lamellar spacing, graphitization degree, aromatic carbon lamellar lateral size, and aromatic carbon lamellar stacking height [10-12]. The changes in these parameters are shown in Figure 7 and will be discussed in detail below. The method for calculating WAXS structural parameters is detailed in the literature [5,16].

mesopores and macropores, resulting in an increase in all pore sizes and rougher pore surfaces. The surface fractal dimension, porosity, and specific surface area all increase, while the basic structure of the carbon skeleton remains stable, with the pore fractal dimension remaining unchanged. The apparent density of coal slightly increases (Table 2). The release of bound water increases electron density fluctuations within the pores, increasing the Porod slope. Changes in the lamellar spacing, the lamellar stacking height, the lamellar lateral size and graphitization degree are negligible. At approximately 200~400°C, anthracite continues to release the majority of bound water and begins decomposing a small number of unstable oxygen-containing functional groups on the aromatic nuclei, releasing gases [1,3]. Porosity and specific surface area slightly increase. The basic structure of the aromatic nuclei in the carbon skeleton remains intact, with fluctuations in the surface fractal dimension, pore fractal dimension, pore distribution, average pore size, Porod slope, and lamellar stacking height. The released gases open up the aromatic layers, causing lamellar spacing and lamellar lateral size to fluctuate upward, and graphitization degree to fluctuate downward.

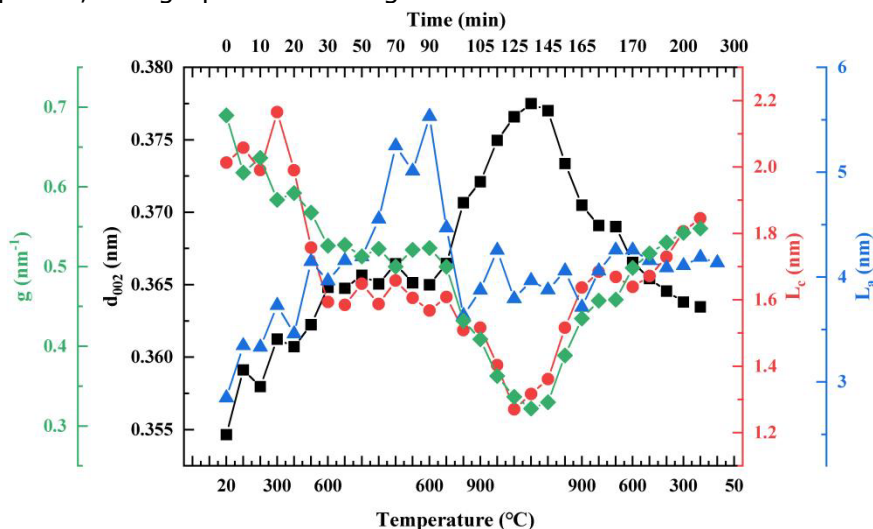


Figure 7. Changes in the structural parameters of graphitic microcrystals during the preparation of activated carbon from anthracite. Parameters include graphitization degree ( $g$ ), lamellar spacing ( $d_{002}$ ), lamellar stacking height ( $L_c$ ), and lamellar lateral size ( $L_a$ ), calculated from WAXS.

(3) **Intense thermal decomposition:** At approximately 400~600°C, the thermal decomposition of anthracite intensifies, breaking down the aliphatic side chains and functional groups around the basic aromatic nuclei, producing coal gas, coal tar, and char [1,3]. More pores are generated and opened within the solid carbon network, with an increase in small pores, mesopores, and macropores, leading to rapid increases in average pore size, surface fractal dimension, pore fractal dimension, porosity, and specific surface area. The continuous generation and release of coal gas and tar cause fluctuations in the Porod slope. Some free radicals begin to combine, elongating the aromatic layers, increasing lamellar lateral size. The released gases and liquids open up the aromatic layers, even causing them to misalign and split, increasing lamellar spacing and decreasing graphitization degree and lamellar stacking height.

(4) **Thermal condensation:** During the 600°C holding period, the production of coal gas and tar gradually decreases [1,3]. Tar undergoes further decomposition and condensation, while char starts to condense and rearrange as the pyrolysis weakens. Under combined effects, the char structure remains relatively stable. Fluctuations in pore distribution, average pore size, surface fractal dimension, pore fractal dimension, porosity, specific surface area, Porod slope, lamellar spacing, graphitization degree, and lamellar stacking height are minimal. Free radicals combine, leading to the reorganization, connection, and growth of aromatic layers, increasing lamellar lateral size.

In summary, during carbonization, the organic matter in anthracite undergoes pyrolysis, carbonization, and reorganization, forming a porous network structure of char, which constitutes the original structural form of activated carbon, namely, a graphitic-like basic microcrystalline structure [1,3]. Voids remain between the microcrystals [2]. At this stage, due to the precipitation and decomposition of tar substances, these voids are occupied or blocked by disordered amorphous carbon. Therefore, the adsorption capacity of the carbonized product is relatively low and requires activation to enrich the pore structure. Additionally, the structural changes in the carbonized material during the holding period are minimal, indicating that the holding time during the carbonization of anthracite can be shortened or even eliminated. The decomposition of minerals during high-temperature carbonization reduces their influence on the final structure of the activated carbon. Although mineral residues may have a minor effect on scattering patterns and interlayer spacing during intermediate stages, the observed changes in graphitic microcrystal spacing are predominantly attributed to the thermal and chemical transformations of the carbon skeleton.

### 3.5. Activation

In this study, the basic activation process involves heating the char formed at 600°C from the carbonization of anthracite in a carbon dioxide atmosphere to 900°C and holding for 1 hour. Carbon dioxide, as an oxidizing atmosphere, primarily functions to create pores [1,3]. As shown in Figures 5 and 7, the activation process of anthracite can be divided into three stages: mild activation, intense activation, and stabilization.

(1) **Mild activation:** At approximately 600~700°C, the decomposition of volatile substances in the char continues, with the rate of pore blockage by coal gas and tar exceeding the rate of pore opening by carbon dioxide and tar reaction [1,3]. The volumes of small pores, mesopores, and macropores decrease, with reductions in average pore size, pore volume, porosity, specific surface area, surface fractal dimension, and pore fractal dimension. The Porod slope increases, lamellar spacing and lamellar stacking height increase, and graphitization degree decreases as lamellar spacing increases. Microcrystals react with carbon dioxide and are burned away, decreasing lamellar lateral size.

(2) **Intense activation:** At approximately 700~900°C, the release of volatile substances in the char nears completion, and the reaction of carbon dioxide with tar, amorphous carbon, and microcrystals becomes dominant [1,3]. Under carbon dioxide activation, tar and other substances within the pores, as well as disordered amorphous carbon, are removed, opening previously blocked pores. Carbon dioxide diffuses into the initial pores, reacting and enlarging them, sometimes causing the walls of adjacent pores to burn away and merge, increasing the volumes of transitional pores and macropores. At this point, the surfaces of the basic microcrystals are exposed and react with the activating agent, causing burn-off. The burn-off of microcrystals is uneven, occurring faster parallel to the carbon layers than perpendicular to them, with a higher reaction rate at edges and defects, leading to the formation of new pores. These reactions increase the volumes of small pores, mesopores, and macropores, with small pores increasing the most, making the pore network more developed and complex. Thus, the pore fractal dimension, porosity, specific surface area, and lamellar spacing increase rapidly, while lamellar stacking height, lamellar lateral size, and graphitization degree decrease rapidly. Carbon dioxide first reacts with protruding active sites on the pore surface, decreasing the surface fractal dimension; then, carbon dioxide burns off microcrystals, creating new small pores, increasing the surface fractal dimension again. The disordered amorphous carbon gradually decreases, reducing the Porod slope.

(3) **Stabilization:** During the holding period at 900°C, carbon dioxide continuously reacts with the char, further developing and evolving the pore structure of the activated carbon [1,3]. Simultaneously, the skeleton undergoes a degree of crystallization, condensation, and rearrangement, gradually reaching equilibrium, forming a relatively stable structure of activated carbon. Therefore, all mentioned structural parameters fluctuate during this holding period but remain overall stable.

During the activation process, the changes in the pore structure of activated carbon include the expansion of small pores, the formation of mesopores, the generation of macropores, and increases in surface area and fractal dimensions [1,3]. The carbon skeleton structure undergoes rearrangement, reorganization, cracking, and extension, and new functional groups may be introduced or existing functional groups altered due to the activating agent. Additionally, based on the changes in structural parameters, the structural changes of activated carbon during the holding period are minimal, indicating that the holding time during the carbon dioxide activation process of anthracite carbonized material can be shortened or even eliminated. Both the carbon skeleton structure and porous characteristics could be changed from 600°C to 900°C. The changes were undoubtedly derived from both the heat treatment itself and the reaction with activation gas. Additionally, in our previous study [5] on Jincheng anthracite under an inert nitrogen atmosphere, we observed similar trends in  $d_{002}$ : an initial increase during heating, peaking at around 1000°C due to thermal expansion, followed by a gradual decrease during cooling as the structure stabilized. The anthracite samples used in that study and the present work have similar elemental compositions, and the consistency in  $d_{002}$  trends highlights the generality of these thermal effects. These findings support the interpretation that the observed  $d_{002}$  changes in this study are driven by the combined effects of thermal expansion and structural rearrangement. The separation and comparison of these two effects need further study in the future.

In the activation process of coal-based activated carbon, CO<sub>2</sub> activation and steam activation each have their own characteristics, and the process conditions, such as temperature, also differ. As a result, different types of activated carbon with unique properties can be prepared to suit various application scenarios. As an exploratory study on the in-situ preparation of coal-based activated carbon, CO<sub>2</sub> was chosen as the activation agent in this work mainly due to its mild activation effect, aiming to achieve a balance in the development of small pores and mesopores.

The activated carbon prepared in this study has a specific surface area of 234 m<sup>2</sup>/cm<sup>3</sup>, which is relatively low. To further enhance pore development, future studies will consider higher activation temperatures or the use of stronger activation agents, such as steam.

### 3.6. Cooling

In this study, after the activation holding period ends, heating is stopped, and the activated carbon is naturally cooled in a carbon dioxide atmosphere. During this period, the structure of the activated carbon may undergo the following changes [34-35]:

(1) **Release of residual gases:** Some gases may remain from the high-temperature activation process. During natural cooling, these residual gases will gradually be released, potentially making some small pores in the channels more accessible or adjusting certain functional groups on the surface.

(2) **Stabilization of pore structure:** The pore structure formed during high-temperature activation may further stabilize during natural cooling. The size and distribution of the pores may slightly adjust to adapt to the new environmental conditions, leading to the redistribution and adjustment of small pores, which affects the pore structure characteristics of the activated carbon.

(3) **Stabilization of crystal structure:** Under high-temperature conditions, some amorphous carbon may convert to crystalline carbon. During natural cooling, the crystal structure of this crystalline carbon may further form and stabilize, affecting the crystalline structure characteristics of the activated carbon.

(4) **Adjustment of surface functional groups:** During activation, some chemical functional groups may form on the surface, such as hydroxyl or carbonyl groups. During natural cooling, these surface functional groups may undergo adjustments, potentially increasing or decreasing the number of functional groups, affecting the surface chemical properties of the activated carbon.

These changes cause fluctuations in all structural parameters calculated in this study but remain overall stable. This indicates that the structure of activated carbon obtained from anthracite using the carbon dioxide activation method can be retained during natural cooling in a carbon dioxide atmosphere without the need to change the cooling atmosphere.

### 3.7. Comparison between nitrogen adsorption and SAXS results

The nitrogen adsorption and SAXS results provide complementary insights into the pore structure evolution from raw anthracite to activated carbon. Nitrogen adsorption primarily measures open pores, while SAXS captures both open and closed pores, offering a more comprehensive view of the material's structural transformation.

The comparison of specific surface area between nitrogen adsorption and SAXS results is summarized in Table 3, and the pore size distribution from nitrogen adsorption is shown in Figure 8.

Table 3. Comparison of specific surface area between nitrogen adsorption and SAXS.

Sample	BET (m <sup>2</sup> /g)	SAXS (m <sup>2</sup> /cm <sup>3</sup> )/(m <sup>2</sup> /g)
Anthracite	13.58	64.58 / 35.88
Activated carbon	30.67	234.23 / 117.06

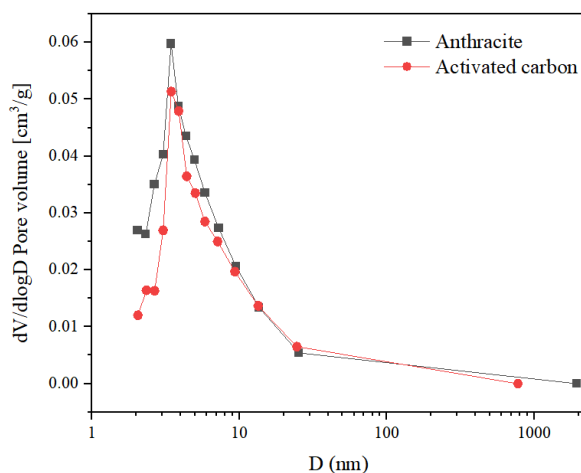


Figure 8. Pore size distribution of anthracite and activated carbon obtained from nitrogen adsorption experiments.

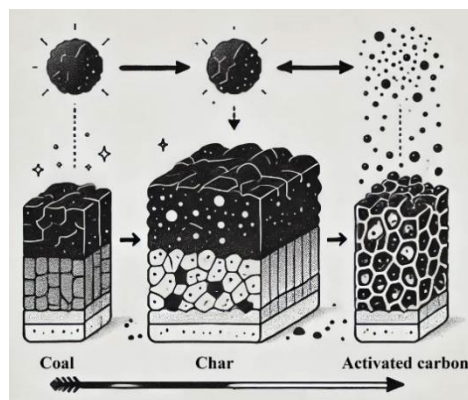


Figure 9. Schematic view of structural evolution from anthracite to activated carbon.

As shown in Table 3, nitrogen adsorption results indicate that raw anthracite has a compact structure with limited open pores, while SAXS reveals the presence of closed pores and/or ink bottle-shaped pores. After activation, nitrogen adsorption detects a significant increase in small pores and mesopores, as shown in Figure 8. SAXS further confirms the development of a more complex pore network, with increased specific surface area and porosity.

However, SAXS results also reveal that the final activated carbon retains many closed pores and/or ink bottle-shaped pores, which nitrogen adsorption cannot directly observe. These pores may result from incomplete activation or structural characteristics that hinder gas penetration. Their presence reduces the fully accessible surface area and may limit adsorption performance.

The combined use of nitrogen adsorption and SAXS highlights the hierarchical pore structure evolution during activation and the potential for further process optimization to address closed pores.

The structural evolution from anthracite to activated carbon can be schematically illustrated as Figure 9. The structure evolution models can be referred in literature [36].

#### 4. Summary

In this study, anthracite from the Zhaogu No. 2 Mine in Jiaozuo, Henan Province, China, was used as the raw material, and carbon dioxide was used as the activating agent to prepare activated carbon. The entire reaction process was studied in situ using SAXS-WAXS based on the Beijing Synchrotron Radiation Facility. The results show that during the preparation of coal-based activated carbon, the structural changes of activated carbon exhibit clear stages. The carbonization process can be roughly divided into four stages: physical desorption, mild thermal decomposition, intense thermal decomposition, and thermal condensation. With increasing temperature, small pores, mesopores, and macropores gradually form, significantly increasing porosity and specific surface area. The activation process can be roughly divided into three stages: mild activation, intense activation, and stabilization. Carbon dioxide further develops the pores, making the pore network structure more complex and developed. Meanwhile, the degree of graphitization of the carbon skeleton decreases during carbonization, decreases first then increases during activation. The cooling process mainly involves the rearrangement and stabilization of microcrystals and pore structures. These changes affect the pore structure characteristics, crystal structure characteristics, and surface chemical properties of the final activated carbon, thereby influencing its adsorption performance and application properties.

The final prepared activated carbon has a high specific surface area and developed pore structure, providing a good structural basis for enhancing its adsorption performance. Additionally, the changes in structural parameters indicate that the holding time during carbonization and carbon dioxide activation of anthracite can be shortened or even eliminated. The structure of activated carbon after high-temperature activation can still be retained during natural cooling in a carbon dioxide atmosphere without the need to change the cooling atmosphere. This study provides experimental insights and practical data support for optimizing the process of preparing high-performance activated carbon from anthracite.

**Acknowledgements:** *This work was supported by the Foundation of State Key Laboratory of Coal Conversion (Grant No. J23-24-612).*

**Disclosure statement:** *No potential conflict of interest was reported by the author(s).*

#### References

- [1] Xie Q, Zhang XL, Liang DC, Cao JY, Liu JC. Directed preparation of coal-based activated carbon: principles, approaches and applications (in Chinese). *Coal science and technology*, 2021; 49: 100-127.
- [2] Martin LG, John WL and Irving W (1984). *Coal science* (volume 3). Academic Press.
- [3] Ma JM and Xu JT (2022). *Functional carbon materials*. UK : IOP Publishing.
- [4] Lv Q, Li. ZH, Liu. LZ, Zhao YX, Li DF, Guo WY, Mo G, Lv BL. In situ SAXS study of fractal structure of non-caking coal during carbonisation. *Phil. Mag. Lett.*, 2021; 101: 60-67.
- [5] Wang YX, Li ZH, Kong J, Chang LP, Zhao YX, Li DF, Lv BL. In situ wide-angle X-ray scattering study on the change of microcrystalline structure in Jincheng anthracite during high-temperature carbonization. *J. Appl. Cryst.*, 2022; 55: 265-270.
- [6] Manivannan A, Chirila M, Giles N, Seehra MS. Microstructure, dangling bonds and impurities in activated carbons. *Carbon*, 1999; 37: 1741-1747.
- [7] Smith JWH, McDonald M, Romero JV, MacDonald L, Lee JR, Dahn JR. Small and wide angle X-ray studies of impregnated activated carbons. *Carbon*, 2014; 75: 420-431.
- [8] Glatter O, Kratky O. *Small angle X-ray scattering*. Academic Press Inc, New York. 1982.
- [9] Bello Lawal Toro, Zhiping Li, Caspar Daniel Adenutsi, et al. Pore structure characterization of a low permeability reservoir using nuclear magnetic resonance, nitrogen adsorption and mercury intrusion capillary pressure. *Petroleum and Coal*, 2018; 60: 330-338.
- [10] Bragg W, Bragg W (1915). *X-Rays and crystal structure*. G. Belland Sons, London.
- [11] Langrord J, Wilson A. Scherrer after sixty years: A survey and some new results in the determination of crystallite size. *J. Appl. Cryst.*, 1978; 11: 102-113.
- [12] Wertz DL, and Quin JL. Wide angle X-ray scattering study of the layering in three of the argonne premium coals. *Fuel*, 2000; 79: 1981-1989.

- [13] Diduszko R, Swiatkowski A, Trznadel BJ. On surface of micropores and fractal dimension of activated carbon determined on the basis of adsorption and SAXS Investigations. *Carbon (New York)*. 2000; 38 (8): 1153 – 1162.
- [14] Xie F, Li ZH, Wang WJ, Li DF, Li ZZ, Lv BL, Hou B. In-situ SAXS study of pore structure during carbonization of non-caking coal briquettes. *Fuel*, 2020; 262: 116547.
- [15] Wang YX, Li ZH, Kong J, Chang LP, Zhao YX, Li DF, Lv BL. In situ change of fractal structure in coal with coking capability during high-temperature carbonisation. *Phil. Mag. Lett.*, 2022; 102: 81-92.
- [16] Wang YX, Li ZH, Kong J, Chang LP. Simultaneous SAXS-WAXS study on coking coal during high temperature carbonization. *Carbon Letters*. 2023; 33: 363-372.
- [17] Wang YX, Huang WF, Li ZH, Chang LP, Li DF, Chen RC, Lv Q, Zhao YX, Lv BL. Small furnace for the small angle X-ray scattering (SAXS) and wide angle X-ray scattering (WAXS) characterization of the high temperature carbonization of coal. *Instrum. Sci. Technol.*, 2021; 49: 445-456.
- [18] Li ZH, Wu ZH, Mo G., Xing XQ, Liu P. A small single X-ray scattering station at Beijing synchrotron radiation facility. *Instrum. Sci. Technol.*, 2014; 42: 128-141.
- [19] Xie F, Li ZH, Li ZZ, Li DF, Gao YX, Wang B. Absolute intensity calibration and application at BSRF SAXS station. *Nucl. Instrum. Meth. A.*, 2018; 900: 64-68.
- [20] Chen RC, Li ZH, Shi Y, Liu LZ, Wang YX, Lv BL. Angle calibration and error analysis of wide-angle X-ray scattering (WAXS) with a one-dimensional linear detector. *Instrum. Sci. Technol.*, 2022; 50: 83-94.
- [21] Hammersley A. FIT2D: a multi-purpose data reduction, analysis and visualization program. *J. Appl. Cryst.*, 2016; 49: 646-652.
- [22] Li ZH. A program for SAXS data processing and analysis. *Chinese Physics C.*, 2013; 37: 110-115.
- [23] Bressler I, Pauw BR, Thünemann AF. McSAS : software for the retrieval of model parameter distributions from scattering patterns. *J. Appl. Cryst.*, 2015; 48: 962-969.
- [24] Tsai WT, Liu SC, Hsieh, CH. Preparation and fuel properties of biochars from the pyrolysis of exhausted coffee residue. *J. Anal. Appl. Pyrolysis*. 2012; 93: 63-67.
- [25] Havelcová M, Bičáková O, Sýkorová I, Weishauptová Z, Melegy A. Characterization of products from pyrolysis of coal with the addition of polyethylene terephthalate. *Fuel Process Technol.*. 2016; 154: 123-131.
- [26] Li ZH, Li YM, Gu YD, Wu D. Determination of true density of coal by atomic distribution function method by X-ray diffraction (in Chinese). *Coal Conversion*, 1996; 19 (3): 51-55.
- [27] Xie F, Li ZH, Wang WJ, Li DF, Li ZZ, Lv BL, Hou B. In-situ SAXS study of pore structure during carbonization of non-caking coal briquettes. *Fuel*, 2020; 262: 116547.
- [28] Xie Q, Yao X, Yang C, Jiang Y, Zhang J. Effect of coalification degree of coals on the porosity of coal-based granular activated carbon prepared by briquetting method. *Journal of China Coal Society*, 2015; 40 (1): 196-202.
- [29] Bale HD, Schmidt P W. Small-angle X-ray-scattering investigation of submicroscopic porosity with fractal properties. *Phys. Rev. Lett.*, 1984; 53 (6): 596-599.
- [30] McMahon PJ, Moss SD. Derivation of infinite-slit-smear small-angle scattering from porous surface and porous mass fractals. *J. Appl. Cryst.*, 1999; 32: 956-962.
- [31] Włochowicz A, Rabiej S. Determination of micropore concentration and size distribution in carbon fibres by the saxs method. *Macromol. Mater. Eng.*, 2003; 190: 187-200.
- [32] Koberstein JT, Morra B, Stein RS. The determination of diffuse-boundary thicknesses of polymers by small-angle X-ray scattering. *J. Appl. Cryst.*, 2010; 13: 34-45.
- [33] Li ZH, Zhao JP, Wu D, Sun YH, Wang J, Liu Y, Sheng WJ, Dong BZ. Correction for Porod's positive deviation in small-angle X-ray scattering (in Chinese). *Journal of Chemistry*, 2000; 58 (9): 1147-1150.
- [34] Wang B, Chen H, Li Y, Si H, Wei H, Guo Z, Gu Z, and Hou D. Properties of activated carbon regulated by rapid cooling treatment after pyrolysis. *Bioresources*, 2019; 14: 7927-7942.
- [35] Tazibet S, Boucheffa Y, Lodewyckx P, Velasco LF, Boutillara Y. Evidence for the effect of the cooling down step on activated carbon adsorption properties. *Micropor. and Mesopor. Mat.*, 2016; 221: 67-75.
- [36] Saurel D, Segalini J, Jauregui M, Pendashteh A, Daffos B, Simon P, Casas-Cabanas M. A saxs outlook on disordered carbonaceous materials for electrochemical energy storage. *Energy Storage Mater.*, 2019; 21: 162-173.

To whom correspondence should be addressed: Dr. Zhihong Li, Beijing Synchrotron Radiation Facility, Institute of High Energy Physics, Chinese Academy of Sciences, Beijing 100049, China, E-mail: [lzh@ihep.ac.cn](mailto:lzh@ihep.ac.cn)